

Physics with Neutrons I

Alexander Backs
alexander.backs@frm2.tum.de

WS 18/19
31.01.2019

Exercise sheet 10

<https://wiki.mlz-garching.de/n-lecture06:index>

Solutions

1. Reverse engineering 'real' data

The following exercise should illustrate, how various effects affect the scattering data and how difficult it can become to interpret data, even for simple models.

Start by considering very dilute spherical particles with a radius $R = 100\text{nm}$. The scattering length density has its maximum value $\Delta\rho_b(0)$ at the center of the particle and falls off linearly to $\Delta\rho_b(R) = 0$ at its edge. (a smoothly varying distribution like this might happen in magnetic particles with a corresponding field distribution).

- Calculate the scattering cross section and take a look at the Guinier and Porod regime. Are they different from a homogeneous sphere?
- Now we introduce polydispersity: the particles have a certain distribution of various sizes. Assume, e.g. a Gaussian distribution centered around R , with a standard deviation $\sigma = 2\%$. (also test how the signal is changing when increasing the size distribution to 10% or higher)
- Additionally, the instrumentation degrades the obtained signal. assume a Gaussian shape of the direct neutron beam with a standard deviation $\sigma = 4 \cdot 10^{-4}/\text{\AA}$ and perform a convolution on the signal.
- As a last step, we implement a 'real' detector, by assuming discrete pixels. For this, bin the data up to $q = 5 \cdot 10^{-2}/\text{\AA}$ into 100 equally spaced data points.

Even though we only look at the radial dependence of the scattering cross section, in a standard SANS setup one obtains a 2D image which is later radially averaged for data treatment. If we are interested in even smaller scattering angles, a common setup is the Bonse-Hart camera, which uses two monochromators (before and after the sample) to increase the angular resolution. However, this technique reduces the 2D data to a 1D data by integrating the radial scattering data over the direction of monochromator rotation axis. So all scattering with the same q component perpendicular to the axis is summed up into a single value. This effect is called slit smearing.

$$\left(\frac{d\sigma(q_x)}{d\Omega}\right)_{slit} = \int \frac{d\sigma(\sqrt{q_x^2 + q_y^2})}{d\Omega} dq_y$$

- Take the scattering curve from step one and calculate, how the obtained signal will change. Again, take a look at the Guinier and Porod regimes.

Solution

The radial scattering length density is given by a linear dependence, where we omit a definit value for $\Delta\rho_{b,0}$ because without a sample volume the Data has to be arbitrarily normalized anyways.

$$\Delta\rho_b(r) = \Delta\rho_{b,0}\left(1 - \frac{r}{R}\right)$$

Inserting this into the Ansatz for a radially symmetric scattering cross section it yields:

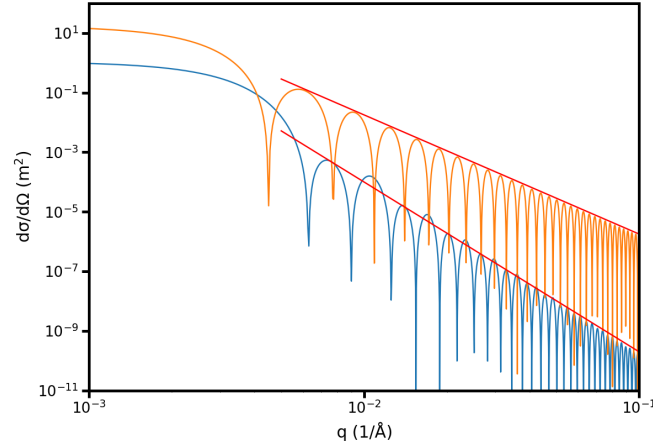
$$\frac{d\sigma}{d\Omega} = 16\pi^2\Delta\rho_{b,0}^2\left(\int_0^R \frac{r}{q} \sin(qr)dr - \int_0^R \frac{r}{R} \frac{r}{q} \sin(qr)dr\right)^2$$

The constant part of $\Delta\rho_b(r)$ gives the same contribution as a homogeneous sphere, which is corrected by the linear term. We use the following integral solutions:

$$\int_0^R \frac{r}{q} \sin(qr)dr = \frac{\sin(qR) - qR \cos(qR)}{q^3}$$

$$\int_0^R \frac{r^2}{q} \sin(qr)dr = \frac{2qR \sin(qR) - (q^2R^2 - 2) \cos(qR) - 2}{q^4}$$

Using these formulas, we can plot the scattering cross section which is shown below (blue), alongside the function of a homogeneous sphere with constant $\Delta\rho_b$ (orange). The most striking differences are the position of the first dip or maximum which is at higher q and indicates a smaller particle size. This is because the scattering length density is higher at a lower radius. Additionally the decay at high q (Porod regime) is faster than q^{-4} with an approximate value of $q^{-5.7}$. This effect represents the very smeared out boundary between particle and solution. The scattering intensity of the sphere is higher (at low q) simply because the integrated scattering length of the particle is higher (the volume is the same, but the sld distribution is different)



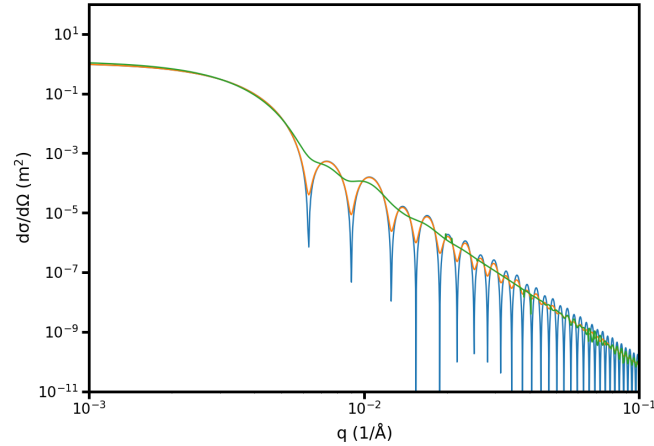
For the next step, to include polydispersity, we perform the average over a size distribution, given by a Gaussian.

$$f(R) = \frac{1}{\sqrt{2\pi}\sigma^2} e^{-\frac{(R-R_0)^2}{2\sigma^2}}$$

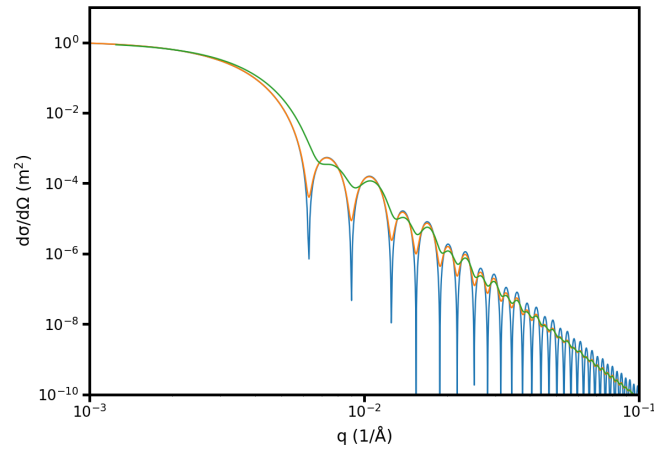
The integration is performed over the scattering cross section after the absolute square. The reasoning for this is, that scattering in a dilute sample is always only happening at a single particle. The detector will then measure the signal of single scatterers with different sizes. If we would perform the average before the absolute square, we would assume that scattered waves from different particles would interfere. Due to the limited correlation length of neutrons, interference effects can only happen for small particles and high concentrations of the solution.

$$\frac{d\sigma}{d\Omega_{poly}} = \int f(R) \frac{d\sigma(R)}{d\Omega} dR$$

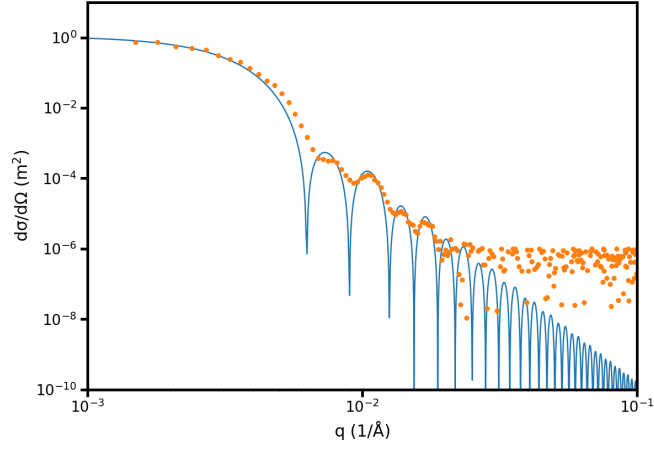
The graph below shows the polydisperse curve for $\sigma = 2$ nm (in orange) and $\sigma = 10$ nm (in green) along with the monodisperse curve in blue. The effect of polydispersity is obviously a smearing of the minima and maxima. For $\sigma = 10$ nm (compared to $R = 100$ nm !) this effect is already so large, that practically no features remain compared to the other curves. Note however, that the low q regime remains nearly unchanged.



To see the effect of instrument smearing we assume we measured the direct beam, again shaped like a Gaussian distribution with $\sigma = 8 \cdot 10^{-4} / \text{\AA}$. In reality, the 2D shape of the direct beam would be convoluted onto the 2D scattering function and then a radial average is performed, but we restrict ourselves to the 1D case for simplicity. The result is shown below, with the original scattering function in blue, the 2% polydisperse signal in orange and the additionally smeared graph in green. Again, as expected, the features become more smeared out, but the effect is slightly different to a higher polydispersity. The low q regime gets changed more, while the oscillation at high q remains visible.



For the last step, the data (polydisperse and smeared by the direct beam) has been binned (summed up) into discrete pixels, with each pixel covering the range of $3 \cdot 10^{-4} / \text{\AA}$. Additionally, a background of $1 \cdot 10^{-6} / \text{\AA}$ and some noise has been added. The data points now resemble a real measurement which should illustrate how difficult it can be to interpret real experiments. Much of the high q information gets lost in background and noise, making it harder to evaluate the Porod law. The low q regime (Guinier) is smeared out and we cannot measure down to $q = 0$. The few features visible in between are altered quite strongly in comparison to the model calculation.



The formula for slit smearing can be rearranged by a simple change of integration variable to make it more usable:

$$\left(\frac{d\sigma(q_x)}{d\Omega}\right)_{slit} = \int_{-\text{inf}}^{\text{inf}} \frac{d\sigma(\sqrt{q_x^2 + q_y^2})}{d\Omega} dq_y$$

$$q_y = \sqrt{q^2 - q_x^2}, \quad \frac{dq_y}{dq} = \frac{q}{\sqrt{q^2 - q_x^2}}$$

$$\left(\frac{d\sigma(q_x)}{d\Omega}\right)_{slit} = 2 \int_{q_x}^{\text{inf}} \frac{q}{\sqrt{q^2 - q_x^2}} \frac{d\sigma(q)}{d\Omega} dq$$

Even for the simple particles we use, the integral is best solved in a numerical way. The result is shown below (orange curve) together with the unsmeared result from above (blue). Major changes are smeared and shifted minima and maxima and a different Porod exponent. The exponent changes due to the integration over one q component.

